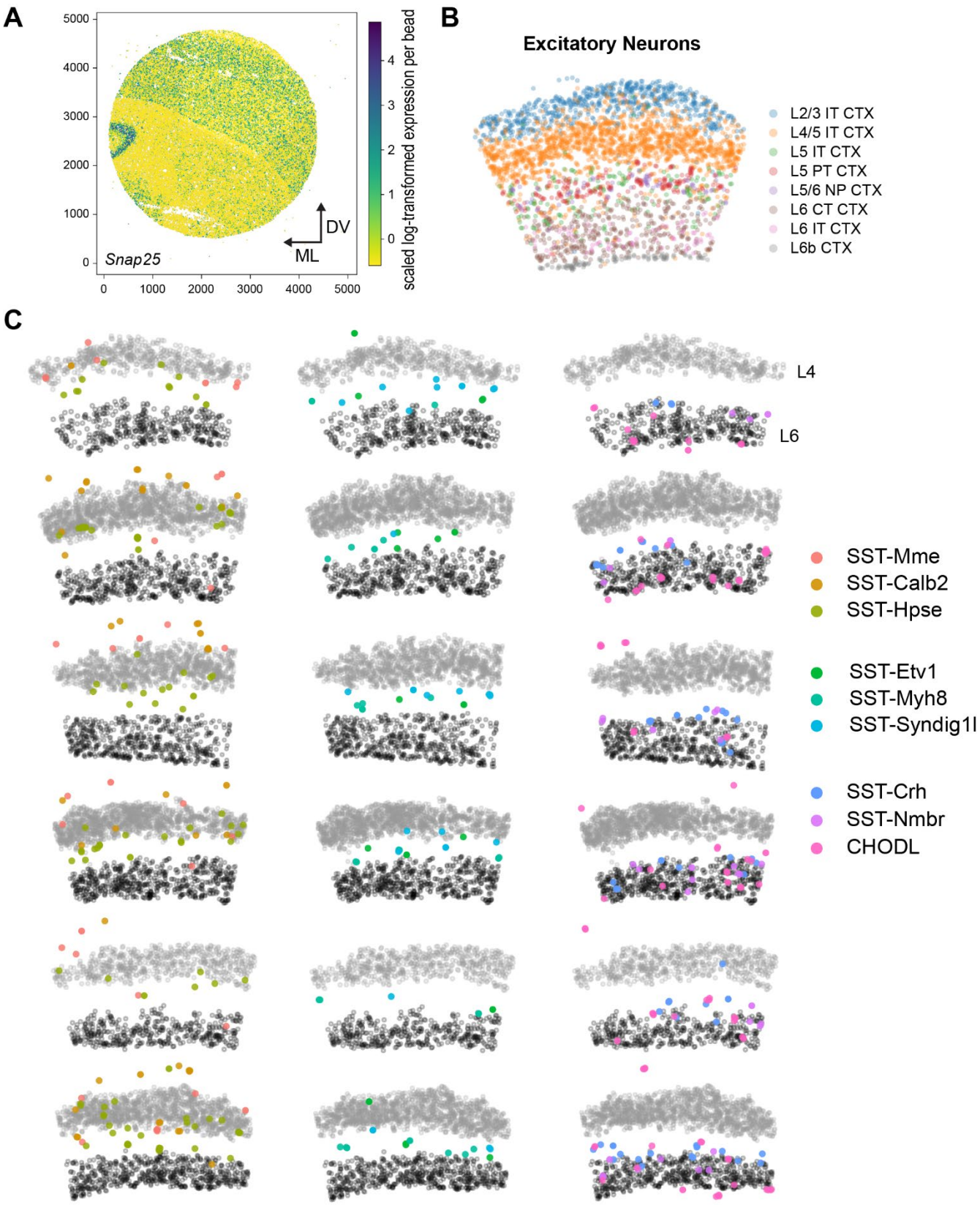

Figure S1. Slide-seq V2 method: identification of cortical region, excitatory neuron assignment and SST subtype distribution in the other six experiments. Related to STAR Method and Figure 1.

(A) Expression of the *Snap25* gene can assist in defining the cortex region in a coronal section of a mouse brain processed by Slide-seq V2 (same experiment as shown in Figure 1C). Each dot represents a bead colored according to the scaled log-transformed expression level of the *Snap25* gene. Any subsequent analysis is restricted to the cortical region where all cortical layers are represented (highlighted region).
(B) Same tissue section as in (A), with dots colored by their predicted identity according to the assignment by robust cell type decomposition (RCTD). Only excitatory neurons are shown.
(C) The rest six Slide-seq V2 experiments in the S1 region with RCTD-predicted SST interneurons labeled. Grey circles showing the location of L4 and L6 excitatory neurons for reference.

Probe Gene Names	*Calb2*	*Hpse*	*Cbln4*	*Pdyn*	*Crh*	*Chodl*
High Expression In	SST-Calb2 CHODL	SST-Hpse	SST-Calb2 SST-Hpse	SST-Syndig1l SST-Hpse	SST-Crh	CHODL
Low Expression In	SST-Mme	SST-Syndig1l	SST-Mme	SST-Calb2 SST-Nmbr	SST-Nmbr	

Table S1. List of smFISH probes and their expression levels in different SST subtypes. Related to Figure 1.

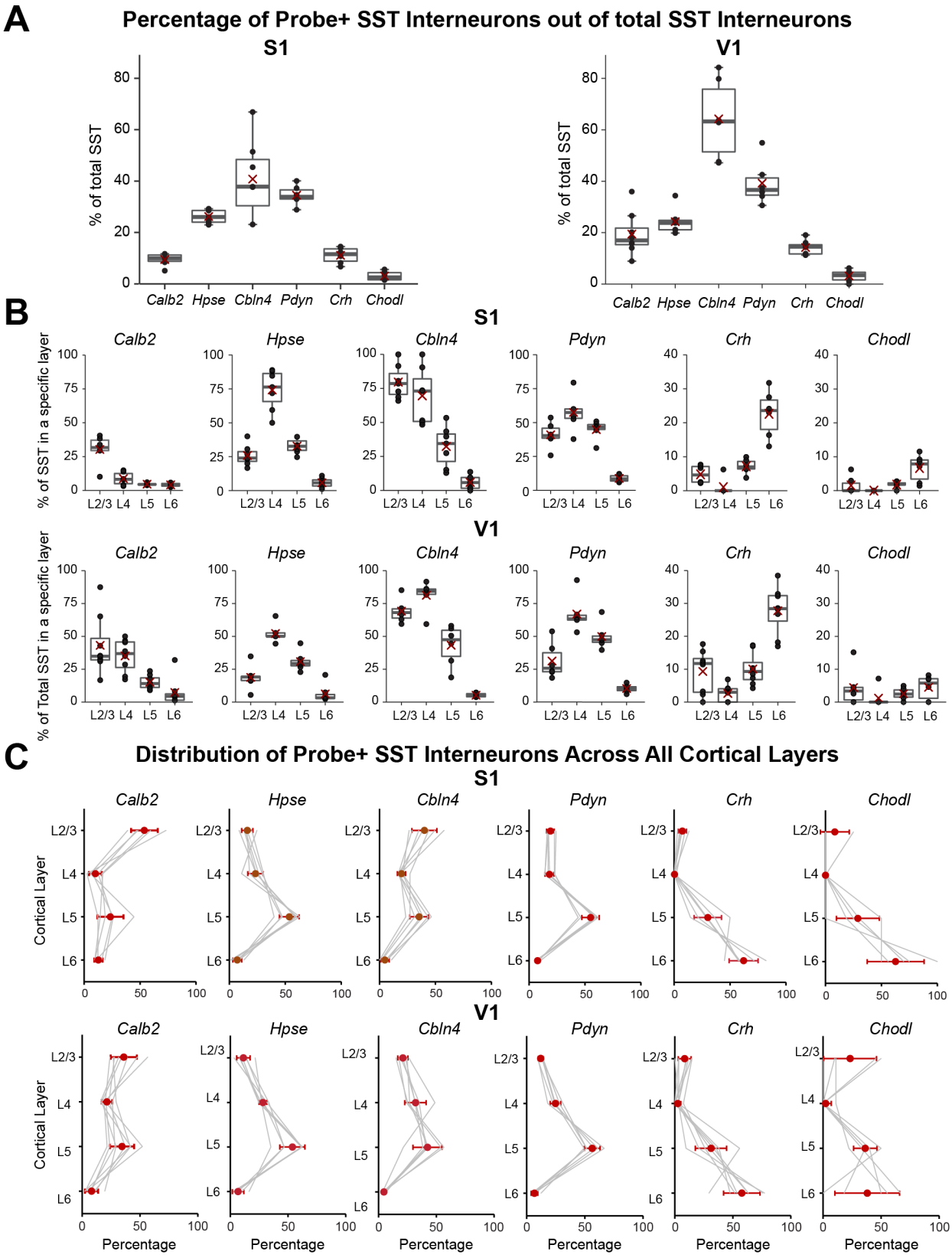

Figure S2. Quantification of smFISH experiments against different marker genes for various SST subtypes. Related to Figure 1.

smFISH experiments against *Calb2*, *Hpse*, *Cbln4*, *Pdyn*, *Crh,* and *Chodl* mRNA were performed on 1-2 month old mice. For the majority of the experiments, total SST interneurons were genetically labeled by Sst^{Cre}*; Ai14* and were visualized by the endogenous fluorescence of tdTomato protein. Alternatively, SST interneurons were labeled either by immunostaining against GFP protein of Sst^{Cre}*; RCE* mice, or by smFISH against *Sst* transcripts. Each data point represents quantification from one experimental image. *Calb2*: n = 3 mice, total 2034 SST interneurons examined in S1; n = 5 mice, total 1866 SST interneurons examined in V1. *Hpse*: n = 4 mice, total 2161 SST interneurons examined in S1; n = 4 mice, total 1784 SST interneurons examined in V1. *Cbln4*: n = 4 mice, total 1649 SST interneurons examined in S1; n = 3 mice, total 822 SST interneurons examined in V1. *Pdyn*: n = 3 mice, total 1892 SST interneurons examined in S1; n = 4 mice, total 1133 SST interneurons examined in V1. *Crh*: n = 3 mice, total 2131 SST interneurons examined in S1; n = 4 mice, total 1676 SST interneurons examined in V1. *Chodl*: n = 3 mice, total 1491 SST interneurons examined in S1; n = 3 mice, total 1176 SST interneurons examined in V1.

(A). Percentage of total SST interneurons in S1 (left) and V1 (right) that express specific marker genes as identified in smFISH experiments. Red crosses represent the mean value.
(B). Percentage of SST interneurons expressing specific marker genes in each layer in S1 (upper row) and V1 (lower row), as identified in smFISH experiments. Red crosses represent the mean value.
(C) The laminar distribution of SST interneurons expressing specific marker genes in S1 (upper row) and V1 (lower row). Red dots with whiskers represent mean ± SD.

SST Subtype	Cell#	Percentage
SST-Mme	196	12.55%
SST-Calb2	307	19.65%
SST-Hpse	230	14.72%
SST-Etv1	41	2.62%
SST-Myh8	221	14.15%
SST-Syndig1l	60	3.84%
SST-Crh	232	14.85%
SST-Nmbr	208	13.32%
CHODL	67	4.29%

Table S2. Proportions of different SST subtypes in the snRNA-seq dataset of P28 cortical interneurons in V1. Related to Figure 1.

SST Subtypes	Genetic Strategy	Boolean Logic
CHODL	*Nos1*^{CreER}; *Sst*^{FlpO}	Cre AND Flp
SST-Calb2 CHODL	*Calb2*^{Cre}; *Sst*^{FlpO}	Cre AND Flp
SST-Etv1 SST-Mme SST-Calb2*	*Etv1*^{CreER}; *Sst*^{FlpO}	Cre AND Flp
SST-Myh8	*Chrna2-Cre*	Cre only
SST-Hpse SST-Calb2	*Pdyn*^{Cre}; *Npy*^{FlpO}	Cre AND Flp
SST-Syndig1l SST-Hpse*	*Pdyn*^{CreER}	Cre only†
SST-Hpse SST-Syndig1l	*Hpse*^{Cre}	Cre only†
SST-Syndig1l	*Pdyn*^{CreER}; *Npy*^{FlpO}	Cre-ON/Flp-OFF
SST-Syndig1l	*Pdyn*^{Cre}; *Npy*^{FlpO}	Cre-ON/Flp-OFF†
SST-Crh	*Crh*^{Cre}; *Sst*^{FlpO}	Cre AND Flp
SST-Nmbr	*Crhr2*^{Cre}; *Sst*^{FlpO}	Cre AND Flp
PV/SST-Th SST-Mme	*Tac1*^{Cre}; *Sst*^{FlpO}	Cre AND Flp

Table S3. Genetic strategies targeting different SST subtypes. Related to Figure 2.

For genetic strategies that target multiple SST subtypes, the list of SST subtypes was arranged with the primary target on the top and the minor target at the bottom. * following specific SST subtype suggests that this subtype was labeled in variable degrees depending on the extent of Cre recombination. † indicates genetic strategies that work only at a certain age range. *Hpse*^{Cre} shows germline recombination. *Pdyn*^{Cre} is expressed in a subset of excitatory neurons during development. Note that although *Crh* gene is expressed in a small subset of SST-Nmbr interneurons. However, due to the low efficacy of *Crh*^{Cre} line in labeling SST-Crh interneurons, we believe the chance of this genetic strategy labeling SST-Nmbr is low. The developmental expression of *Tac1* gene in PV/SST-Th subtype caused the labeling of L6 interneurons of this intersectional strategy.

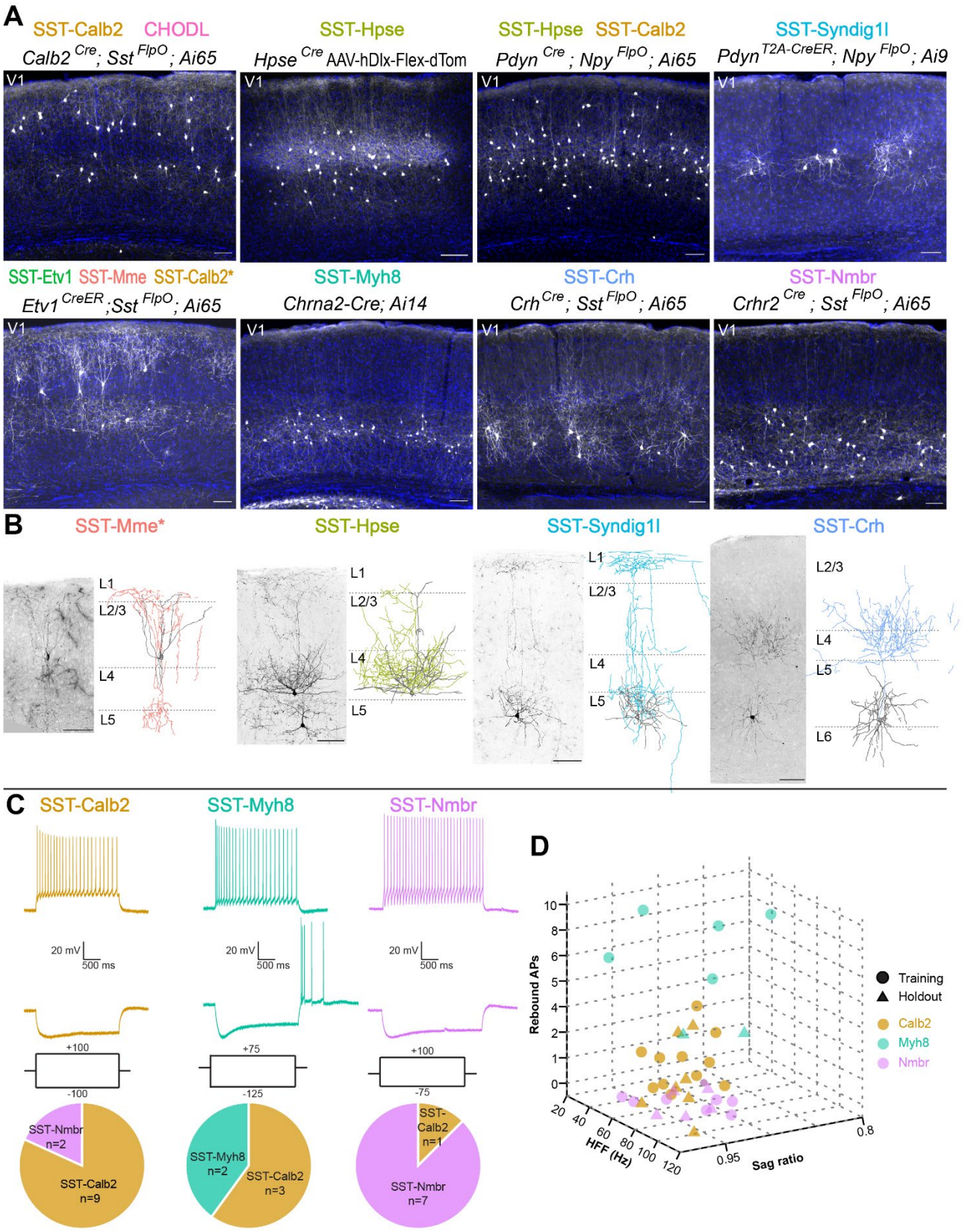

Figure S3. Genetic labeling and single-neuron reconstruction of selected SST subtypes in V1; intrinsic electrophysiological properties of three SST subtypes in S1. Related to Figure 2.

(A) Representative images of selective genetic strategies targeting SST subtypes in V1, with DAPI counterstaining for laminar distribution. All images were taken from 1-3 month old mice. The *Ai9* reporter line is used here as a Cre-ON/Flp-OFF strategy because the FRT sites flanking the mutation are still retained in this mouse line. With this reporter line, SST-Hpse interneurons were occasionally observed in $Pdyn^{T2A\text{-}CreER}$; Npy^{FlpO}; *Ai9* strategy, likely due to incomplete FlpO recombination, though not noted in this representative image. For SST-Hpse labeling, rAAV9-hDlx-Flex-dTomato virus was stereotaxically injected in $Hpse^{Cre}$ mice in V1 at 1 month old and examined 13 days post-injection. * indicates that SST-Calb2 interneurons may be present in this example (see also Figure S5B). Scale bars, 100 µm.
(B) Sparse labeling of selective SST subtypes in V1. Images of genetic labeling are shown to the left of the Neurolucida reconstruction of single-neuron morphology. *Note that the example of SST-Mme sparse labeling was targeted by the intersectional strategy of $Etv1^{CreER}$; Sst^{FlpO}; *RC::FPSit*, which could also label SST-Etv1 and a varying degree of SST-Calb2. Because this example neuron resides in L2/3, whereas SST-Etv1 interneurons are expected to primarily reside in L5a, and that the chance of labeling SST-Calb2 is relatively low due to the low level of recombination, we infer that the identity of this labeled neuron is most likely SST-Mme. SST-Hpse and SST-Syndig1l interneurons are both labeled by $Pdyn^{T2A\text{-}CreER}$; *Ai14* strategy and differentiated by their unique morphology. SST-Crh interneuron is labeled by Crh^{Cre}; Sst^{FlpO};*RC::FPSit*. All reconstructions were derived using sparse labeling of specific SST subtypes from P25-73 mice. Scale bars, 100 µm.
(C) Representative traces of three SST subtypes in response to current injections. SST-Calb2 (n = 21, 3 mice), SST-Myh8 (n = 12, 3 mice), and SST-Nmbr (n = 13, 3 mice) all showed regular-spiking adapting firing patterns (top). Pie charts showing the number of cells classified as SST-Calb2, SST-Myh8, and SST-Nmbr interneurons by a trained k-nearest neighbor classifier (bottom, from left to right). Also see Table S5-6.
(D) 3D plot of the three most predictive features in the nearest neighbor analysis.

SST Subtype	Adult Marker Genes	Resident Layer	Axonal Project Pattern	Putative Cell Type	Tasic *et al.*, 2018 clusters
SST-Mme	*Tac1, Necab1, Fam43a*	L2/3	L1, L2/3	Martinotti cell	Sst Tac1 Tacr3 Sst Tac1 Htr1d Sst Mme Fam114a1
SST-Calb2	*Pcsk5*	L2/3, L5a (S1) L2/3, L4, L5a (V1)	L1, L2/3	Fanning-out Martinotti cell	Sst Calb2 Pdlim5 Sst Calb2 Necab1
SST-Hpse	*Ascl2*	L4, L5a	L4	L4-targeting non-Marinotti cell	Sst Hpse Cbln4
SST-Etv1	*Mstn*	L5	L1, L2/3	Martinotti cell	Sst Nr2f2 Necab1 Sst Myh8 Etv1
SST-Myh8	*Chrna2, Plpp4, Cartpt, Myh13, Glra3*	L5b	L1, L5	T-shaped Martinotti cell	Sst Chrna2 Glra3 Sst Myh8 Fibin Sst Myh8 Etv1 Sst Chrna2 Ptgdr
SST-Syndig1l	*C1qtnf7, Pdyn, Prdm1*	L5a	L1	T-shaped Martinotti cell	Sst Hpse Sema3c Sst Chrna2 Ptgdr
SST-Crh	*Rxfp1, Prdm8, Ptprk, Lmo1*	L5b, L6	L4, L5/6	L4-targeting non-Marinotti cell	Sst Rxfp1 Prdm8 Sst Rxfp1 Eya1 Sst Tac2 Tacstd2
SST-Nmbr	*Lpar1, Esm1, Crhr2*	L6	L5/6	L5/6-targeting non-Martinotti cell	Sst Crh 4930553C11Rik Sst Crhr2 Efemp1 Sst Esm1 Sst Tac2 Myh4
CHODL	*Nos1, Sfrp1, Ntn1, Rasgef1b, Carhsp1*	L6	L6, long-range	*Nos1*$^+$ non-Martinotti, long-range projecting neuron	Sst Chodl

Table S4. Summary of the current understanding about different SST subtypes. Related to Figure 2.

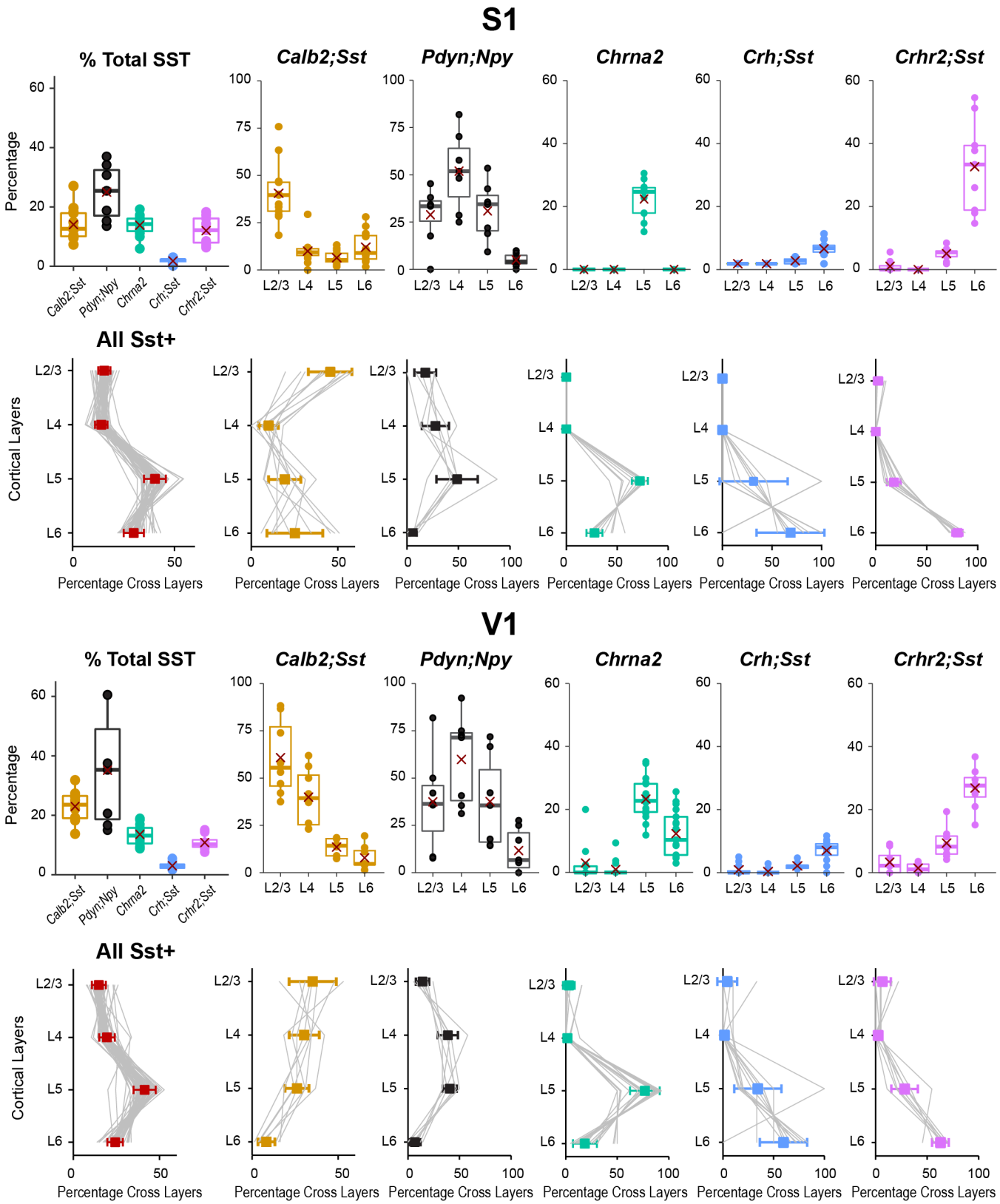
S1
% Total SST
Calb2;Sst
Pdyn;Npy
Chrna2
Crh;Sst
Crhr2;Sst
Percentage
Calb2;Sst
Pdyn;Npy
Chrna2
Crh;Sst
Crhr2;Sst
L2/3
L4
L5
L6
All Sst+
Cortical Layers
Percentage Cross Layers
V1
% Total SST
Calb2;Sst
Pdyn;Npy
Chrna2
Crh;Sst
Crhr2;Sst
Percentage
Calb2;Sst
Pdyn;Npy
Chrna2
Crh;Sst
Crhr2;Sst
L2/3
L4
L5
L6
All Sst+
Cortical Layers
Percentage Cross Layers

Figure S4. Proportion and distribution of SST subtypes across cortical layers in S1 and V1. Related to Figure 2.

Total SST interneurons were labeled with smFISH against *Sst* mRNA. Genetic labeling was visualized either by endogenous fluorescence or by immunostaining against reporter protein. All experiments were performed on 1-2 month old transgenic mice. Each data point represents quantification from one experimental image.
Calb2^{Cre}; Sst^{FlpO}; Ai65: 4 mice, total 4042 SST interneurons examined in S1; 4 mice, total 1090 SST interneurons examined in V1.
Pdyn^{Cre}; Npy^{FlpO}; Ai65: 3 mice, total 1352 SST interneurons examined in S1; 3 mice, total 775 SST interneurons examined in V1.
Chrna2-Cre; Ai14: 4 mice, total 3364 SST interneurons examined in S1; 6 mice, total 2446 SST interneurons examined in V1.
Crh^{Cre}; Sst^{FlpO}; Ai65: 3 mice, total 5314 SST interneurons examined in S1; 3 mice, total 3793 SST interneurons examined in V1.
Crhr2^{Cre}; Sst^{FlpO}; Ai65: 4 mice, total 2519 SST interneurons examined in S1; 4 mice, total 1613 SST interneurons examined in V1.

(S1, top row) The proportion of genetically labeled neurons out of total SST interneurons (leftmost) or SST interneurons in each layer (rest) in S1.
(S1, second row) Laminar distribution of all SST interneurons (leftmost) or genetically labeled neurons by each strategy (rest) in S1.
(V1) Parallel quantifications performed in V1.

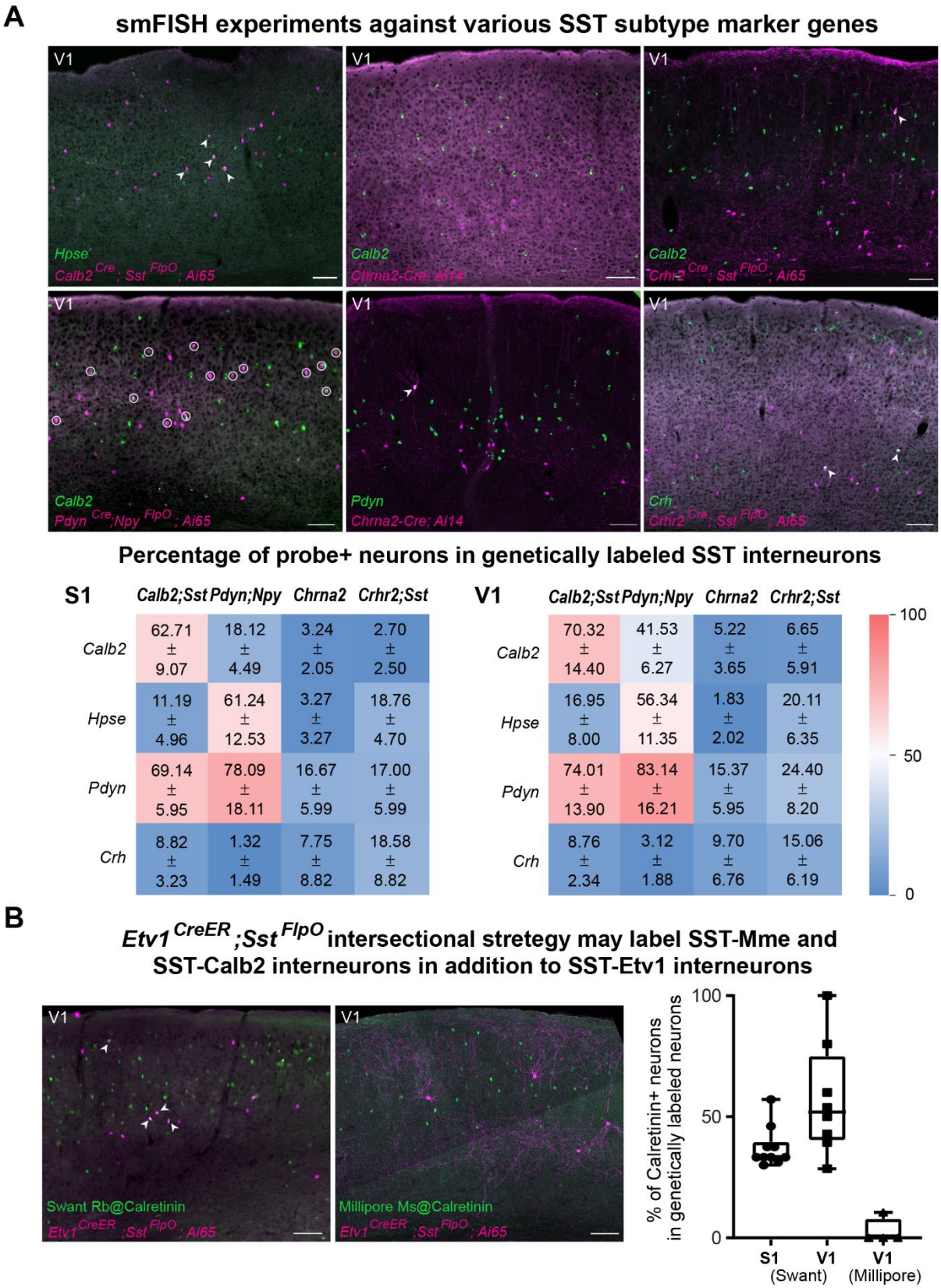

Figure S5. smFISH experiments against various marker genes for assessing the specificity of genetic targeting strategies. Related to Figure 2.

(A) Representative images of smFISH experiments against various marker genes on genetically labeled SST interneurons in V1. Circles or arrows indicating genetically labeled neurons (endogenous fluorescence, magenta) that are positive for the probe (green) against different genes. Scale bars, 100 μm. Heatmaps show the percentage (mean ± SD) of genetically labeled SST interneurons that showed probe expression in S1 and V1. All experiments were performed on 1-3 month old mice.
Calb2^{Cre}; Sst^{FlpO}; Ai65 - *Calb2* probe: 3 mice, 287 genetically labeled neurons examined in S1; 3 mice, 346 neurons in V1. *Hpse* probe: 3 mice, 296 neurons in S1; 3 mice, 414 neurons in V1. *Pdyn* probe: 3 mice, 328 neurons in S1; 3 mice; 288 neurons in V1. *Crh* probe: 3 mice, 278 neurons in S1; 3 mice, 364 neurons in V1.
Pdyn^{Cre}; Npy^{FlpO}; Ai65 – Calb2 probe: 3 mice, 376 neurons in S1; 4 mice, 286 neurons in V1. *Hpse* probe: 5 mice, 846 neurons in S1; 4 mice, 280 neurons in V1. *Pdyn* probe: 5 mice, 630 neurons in S1; 4 mice, 341 neurons in V1. *Crh* probe: 3 mice, 364 neurons in S1; 3 mice, 247 neurons in V1.
Chrna2-Cre; Ai14 – Calb2 probe: 3 mice, 255 neurons in S1; 3 mice, 230 neurons in V1. *Hpse* probe: 4 mice, 393 neurons in S1; 3 mice, 150 neurons in V1. *Pdyn* probe: 3 mice, 420 neurons in S1; 4 mice, 303 neurons in V1. *Crh* probe: 3 mice, 266 neurons in S1; 3 mice, 198 neurons in V1.
Crhr2^{Cre}; Sst^{FlpO}; Ai65 – Calb2 probe: 3 mice, 360 neurons in S1; 4 mice, 321 neurons in V1. *Hpse* probe: 3 mice, 227 neurons in S1; 3 mice, 230 neurons in V1. *Pdyn* probe: 4 mice, 361 neurons in S1; 4 mice, 164 neurons in V1. *Crh* probe: 4 mice, 290 neurons in S1; 5 mice, 406 neurons in V1.
(B) Immunostaining against calretinin with two different antibodies showed different degrees of overlapping with genetically labeled SST interneurons. Arrows indicating genetically labeled neurons that are immunopositive for calretinin. Scale bars, 100 μm. Calretinin antibody from Swant labeled many more neurons than the antibody from Millipore. *Etv1^{CreER}; Sst^{FlpO}* genetic strategy showed little overlapping using Millipore anti-calretinin antibody but ~50% overlapping using Swant antibody, suggesting that this genetic strategy likely labels SST interneurons with a low expression of calretinin. Since SST-Mme interneurons express a low level of calretinin, *Etv1^{CreER}; Sst^{FlpO}* genetic strategy likely labels SST-Mme interneurons besides SST-Etv1 interneurons. Furthermore, because this genetic strategy could label a variable amount of SST interneurons depending on the extent of recombination, it is possible that some SST-Calb2 interneurons are also labeled by this genetic strategy with a high degree of recombination. Swant antibody: 3 mice, 108 genetically labeled neurons examined in S1; 2 mice, 94 genetically labeled neurons examined in V1. Millipore antibody: 2 mice, 52 genetically labeled neurons examined in V1. Experiments were performed on 3-month-old mice.

Parameter	SST-Calb2 mean ± SD n = 21	SST-Myh8 mean ± SD n = 12	SST-Nmbr mean ± SD n = 13	p Value
Vrest (mV)	53.26 ± 0.84	47.27 ± 1.28	57.65 ± 0.95	**<.0001**
IR (MΩ)	311.09 ± 12.25	323.64 ± 23.39	256.73 ± 24.63	.097
Sag ratio	0.92 ± 0.01	0.91 ± 0.01	0.93 ± 0.01	.128
AP Amplitude (mV)	110.46 ± 1.98	97.63 ± 2.7	107.14 ± 3.78	**.007**
AP Half-Width (ms)	1.07 ± 0.05	1.32 ± 0.1	1.02 ± 0.08	**.029**
AP Max Rise (mV/ms)	316.39 ± 14.6	230.20 ± 23.52	290.08 ± 29.98	**.025**
AHP Amplitude (mV)	14.68 ± 1.23	12.69 ± 1.36	16.83 ± 1.48	.177
AP Threshold (mV)	40.40 ± 0.49	38.99 ± 1.26	38.93 ± 1.03	.213
HFF (hZ)	52 ± 3.87	48.58 ± 6.3	74 ± 4.64	**.004**
Adaptation	2.20 ± 0.14	2.26 ± 0.12	1.69 ± 0.14	**.042**
Rebound APs	1.48 ± 0.46	6.42 ± 0.61	0 ± 0	**<.0001**

Table S5. Electrophysiological properties of SST-Calb2, SST-Myh8, and SST-Nmbr interneurons in S1. Related to Figure S3.

Mean ± SEM is reported for all electrophysiology parameters measured. The p-value of the F statistic reports which parameters showed significantly different distributions by one-way ANOVA. Individual mean comparisons with Tukey correction: Vrest: SST-Calb2 vs. SST-Myh8 $p = .0002$, SST-Calb2 vs. SST-Nmbr $p = .01$, SST-Myh8 vs. SST-Nmbr $p < .0001$; AP Amplitude: SST-Calb2 vs. SST-Myh8 $p = .005$; AP halfwidth: SST-Myh8 vs. SST-Nmbr $p = .04$; AP Max Rise: SST-Calb2 vs. SST-Myh8 $p = .02$; HFF: SST-Calb2 vs. SST-Nmbr $p = .02$, SST-Myh8 vs. SST-Nmbr $p = .006$; Adaptation: SST-Myh8 vs. SST-Nmbr $p = .03$; Rebound APs: SST-Calb2 vs. SST-Nmbr $p < .0001$, SST-Calb2 vs. SST-Nmbr $p = .02$, SST-Myh8 vs. SST-Nmbr $p < .0001$.

Parameter	L2/3 SST-Calb2 mean ± SD n = 10	L5a SST-Calb2 mean ± SD n = 11	p Value
Vrest (mV)	52.26 ± 1.03	54.17 ± 1.28	.266
IR (MΩ)	329.43 ± 22.67	294.42 ± 30.66	.377
Sag ratio	0.91 ± 0.01	0.92 ± 0.01	.274
AP Amplitude (mV)	110.39 ± 2.78	110.53 ± 2.94	.973
AP Half-Width (ms)	1.09 ± 0.08	1.05 ± 0.05	.720
AP Max Rise (mV/ms)	316.28 ± 23.94	316.49 ± 18.57	.994
AHP Amplitude (mV)	15.81 ± 1.74	13.65 ± 1.76	.395
AP Threshold (mV)	40.10 ± 0.58	40.68 ± 0.8	.570
HFF (hZ)	51.9 ± 7.42	52.09 ± 3.5	.981
Adaptation	1.88 ± 0.14	2.46 ± 0.19	**.037**
Rebound APs	1.7 ± 0.63	1.27 ± 0.68	.652

Table S6. Electrophysiological properties of SST-Calb2 interneurons in L2/3 and L5 in S1. Related to Figure S3.

Mean ± SEM is reported for all electrophysiology parameters measured. The p-value reports which parameters were significantly different across layers by t-test.

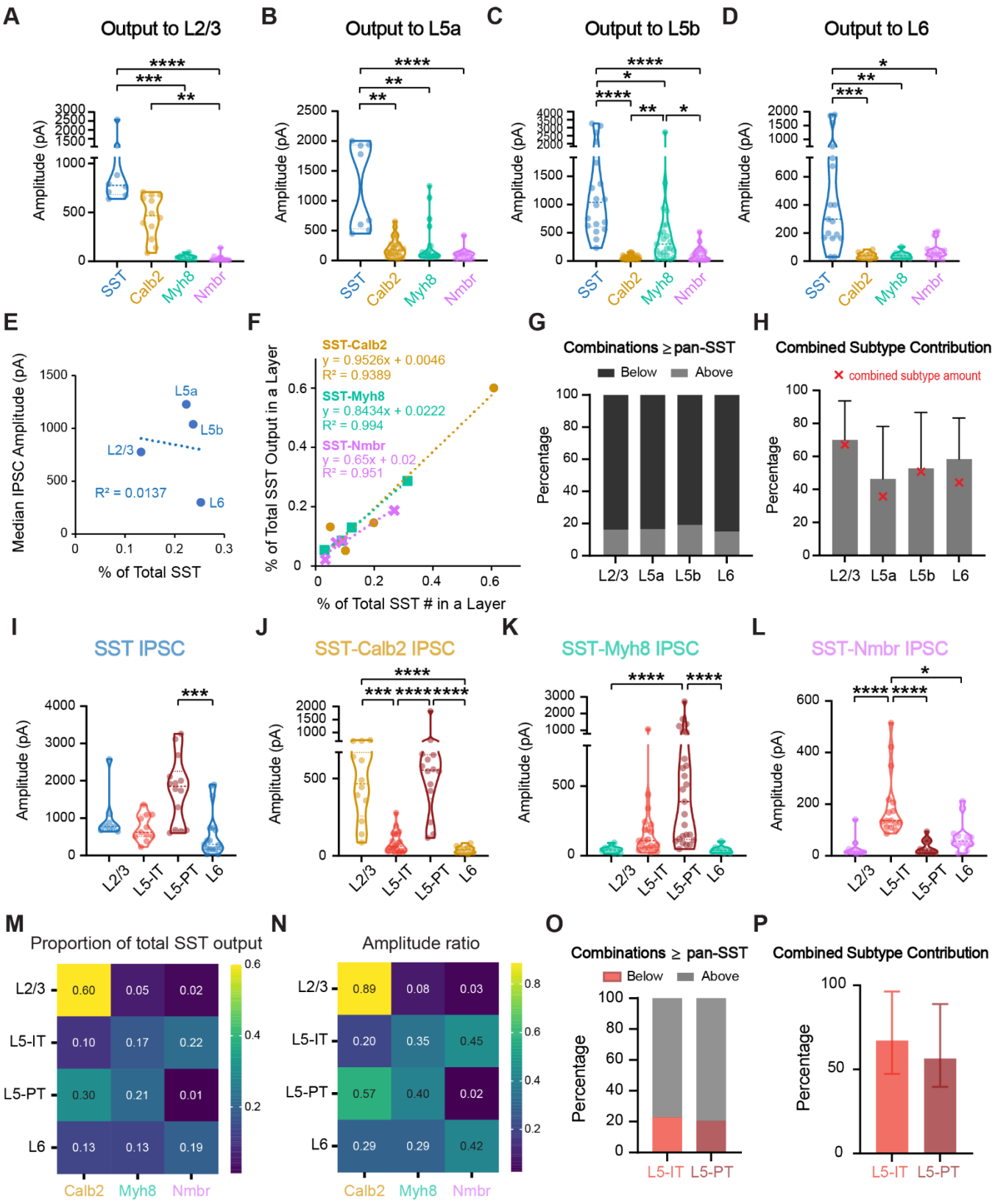

Figure S6. Pyramidal neurons receive laminar and cell-type specific input from different SST subtypes. Related to Figure 3 and Figure 4.

(A) Violin plot of evoked IPSC in L2/3 pyramidal neurons (pan-SST n = 8, 3 mice; SST-Calb2: n = 12, 7 mice; SST-Myh8: n = 8, 5 mice; SST-Nmbr: n = 10, 6 mice). Pan-SST interneuron response was not significantly greater than SST-Calb2 ($p = .5437$) but was greater than SST-Myh8 ($p = .0008$) and SST-Nmbr ($p < .0001$). SST-Calb2 was significantly greater than SST-Nmbr ($p = .0016$). Kruskal-Wallis test with Dunn's correction.
(B) Evoked IPSC in L5a pyramidal neurons (pan-SST: n = 8, 4 mice; SST-Calb2: n = 24, 8 mice; SST-Myh8: n = 20, 7 mice; SST-Nmbr: n = 14, 5 mice). Pan-SST interneuron response was greater than all three subtypes (pan-SST vs. SST-Calb2 $p = .0079$, vs. SST-Myh8 $p = .0012$, vs. SST-Nmbr $p < .0001$). Kruskal-Wallis test with Dunn's correction.
(C) Evoked IPSC in L5b pyramidal neurons (pan-SST: n = 18, 6 mice; SST-Calb2: n = 24, 9 mice; SST-Myh8: n = 23, 7 mice; SST-Nmbr: n = 20, 6 mice). Pan-SST interneuron response was greater than all three subtypes (pan-SST vs. SST-Calb2 $p < .0001$, vs. SST-Myh8 $p = .0349$, vs. SST-Nmbr $p < .0001$). SST-Myh8 response was significantly greater than SST-Calb2 ($p = .0011$) and SST-Nmbr ($p = .0195$). Kruskal-Wallis test with Dunn's correction.
(D) Evoked IPSC in L6 pyramidal neurons (pan-SST: n = 17, 5 mice; SST-Calb2: n = 10, 4 mice; SST-Myh8: n = 8, 5 mice; SST-Nmbr: n = 13, 5 mice). Pan-SST interneuron response was greater than all three subtypes (pan-SST vs. SST-Calb2 $p = .0004$, vs. SST-Myh8 $p = .0017$, vs. SST-Nmbr $p = .0170$). Kruskal-Wallis test with Dunn's correction.
(E) Percentage of the number of SST interneurons residing in a particular layer out of the total number of SST interneurons does not correlate with the percentage of the inhibitory output by total SST interneurons in each layer.
(F) Same plot as Figure 3I with data points from different SST subtypes separately labeled.
(G) Random combinations of SST-Calb2, SST-Myh8, and SST-Nmbr IPSC amplitudes were combined and compared to a pan-SST evoked IPSC amplitude (see STAR Methods). Graph of the percent of simulations where the difference was below (light grey) and above (dark grey) zero.
(H) The proportion of the pan-SST response accounted for by a linear combination of SST-Calb2, SST-Myh8, and SST-Nmbr inputs. Graph of median ratios. Error bars are interquartile ranges. Red crosses indicate the percentage of the combined amount of three SST subtypes out of the total SST interneurons in each layer.
(I) Quantification of the evoked IPSC amplitude upon pan-SST stimulation across pyramidal neuron types (L2/3: n = 8, 3 mice; L5-IT: n = 11, 3 mice; L5-PT: n = 14, 3 mice; L6: n = 17, 5 mice). L5-PT IPSC was significantly greater than L6 ($p = .0003$), all other comparisons not significant (L2/3 vs. L6 $p = .1634$, L5-IT vs. L5-PT $p = .0641$, rest $p > .9999$). Kruskal-Wallis test with Dunn's correction.
(J) As in (I) for SST-Calb2 interneurons (L2/3: n = 12, 7 mice; L5-IT: n = 21, 5 mice, L5-PT: n = 14, 3 mice; L6: n = 10, 4 mice). IPSC was significantly greater in L2/3 and L5-PT neurons than L5-IT or L6 neurons (L2/3 vs. L5-IT $p = .0007$, L2/3 vs. L6 $p < .0001$, L5-PT vs. L5-IT and L5-PT vs. L6 $p < .0001$). Kruskal-Wallis test with Dunn's correction.
(K) As in (I) for SST-Myh8 interneurons (L2/3: n = 8, 5 mice; L5-IT: n = 20, 3 mice; L5-PT: n = 25, 4 mice; L6: n = 8, 5 mice). IPSCs in L5-PT neurons were significantly greater than that L2/3 and L6 (L2/3 vs. L5-PT, L5-PT vs. L6, $p < .0001$). Kruskal-Wallis test with Dunn's correction.
(L) As in (I) but for SST-Nmbr interneurons (L2/3: n = 10, 6 mice; L5-IT: n = 16, 3 mice; L5-PT: n = 14, 3 mice; L6: n = 13, 5 mice). IPSC in L5-IT neurons was significantly greater than in all other cell types (L2/3 vs. L5-IT $p < .0001$, L5-IT vs. L5-PT $p < .0001$, L5-IT vs. L6 $p = .0307$). Kruskal-Wallis test with Dunn's correction.
(M) Heatmap of the proportion of inhibition from individual SST subtype as compared to the inhibition from pan-SST interneurons in different layers and pyramidal neuron cell types.

(N) The ratio of IPCS amplitude for each SST subtype, out of the sum of the three SST subtypes. The combined median IPSC amplitude of the three subtypes is normalized to 1 for a particular layer or pyramidal neuron cell type.
(O) Random combinations of SST-Calb2, SST-Myh8, and SST-Nmbr IPSC amplitudes were combined and compared to a pan-SST evoked IPSC amplitude (see STAR Methods). Graph of the percentage of simulations where the difference was below (pink/red) and above (grey) zero.
(P) The proportion of the pan-SST response accounted for by a linear combination of SST-Calb2, SST-Myh8, and SST-Nmbr outputs. Graph of median ratios. Error bars are interquartile ranges.

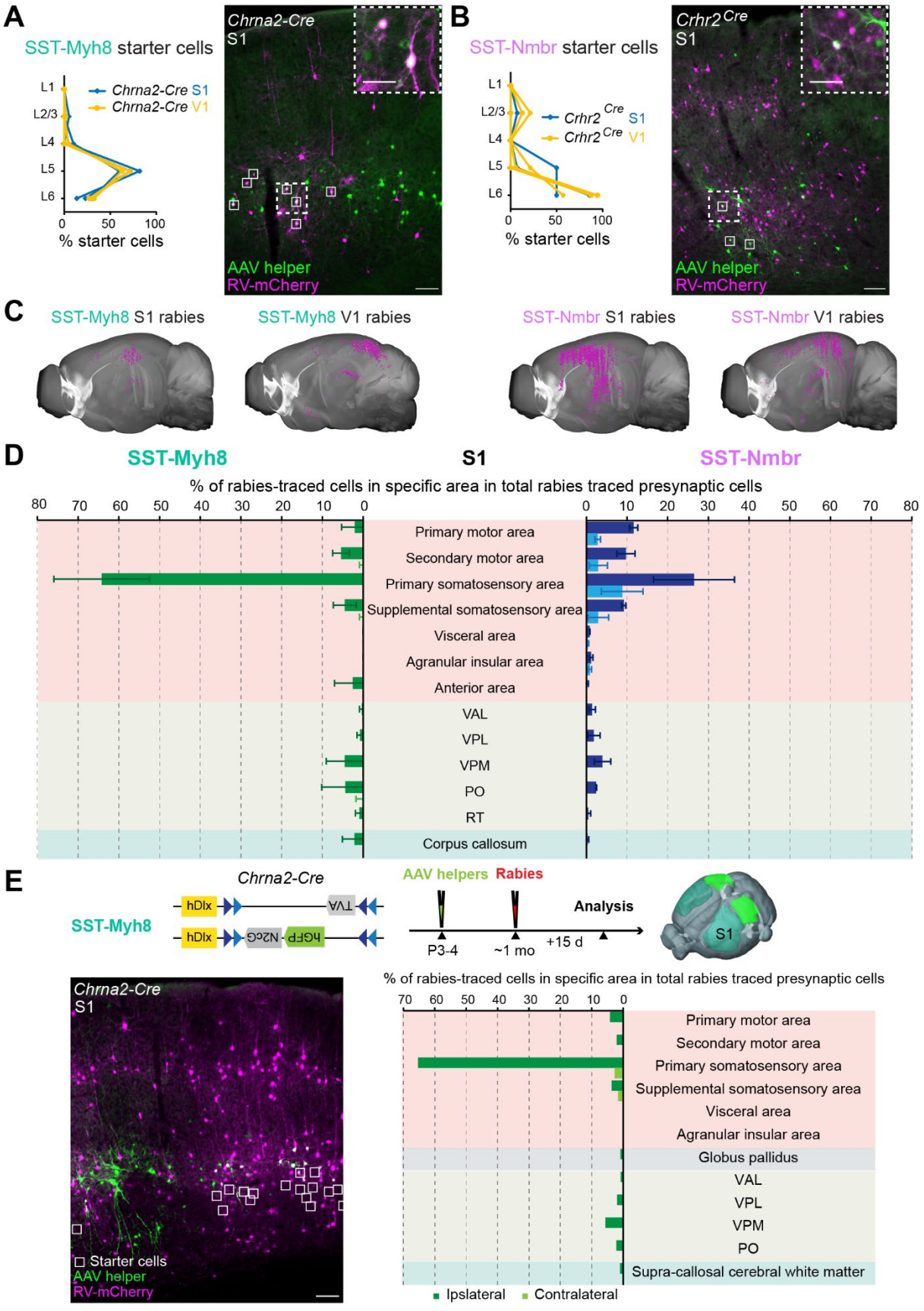
A
SST-Myh8 starter cells
L1
L2/3
L4
L5
L6
Chrna2-Cre S1
Chrna2-Cre V1
0
50
100
% starter cells
Chrna2-Cre
S1
AAV helper
RV-mCherry
B
SST-Nmbr starter cells
Crhr2 Cre S1
Crhr2 Cre V1
% starter cells
Crhr2 Cre
S1
AAV helper
RV-mCherry
C
SST-Myh8 S1 rabies
SST-Myh8 V1 rabies
SST-Nmbr S1 rabies
SST-Nmbr V1 rabies
D
SST-Myh8
S1
SST-Nmbr
% of rabies-traced cells in specific area in total rabies traced presynaptic cells
80 70 60 50 40 30 20 10 0
0 10 20 30 40 50 60 70 80
Primary motor area
Secondary motor area
Primary somatosensory area
Supplemental somatosensory area
Visceral area
Agranular insular area
Anterior area
VAL
VPL
VPM
PO
RT
Corpus callosum
E
Chrna2-Cre
SST-Myh8
hDlx
TVA
hDlx
hGFP-N2cG
AAV helpers
Rabies
Analysis
P3-4
~1 mo
+15 d
S1
Chrna2-Cre
S1
Starter cells
AAV helper
RV-mCherry
% of rabies-traced cells in specific area in total rabies traced presynaptic cells
70 60 50 40 30 20 10 0
Primary motor area
Secondary motor area
Primary somatosensory area
Supplemental somatosensory area
Visceral area
Agranular insular area
Globus pallidus
VAL
VPL
VPM
PO
Supra-callosal cerebral white matter
Ipslateral
Contralateral

Figure S7. Monosynaptic rabies tracing stater cells, rabies tracing results in S1, and one test experiment using the matching AAV helper viruses for rabies tracing from SST-Myh8 subtype as used for SST-Nmbr interneurons. Related to Figure 6.

(A) Laminar distribution of rabies-infected starter cells for rabies tracing experiments from SST-Myh8 and SST-Nmbr interneurons in S1 and V1 (left). Representative images showing starter cells of SST-Myh8 and SST-Nmbr interneurons (right). Neurons expressing AAV-helpers are in green, Rabies (RV) in magenta and starter cells (squares) are identified by both channels. Scale bar, 100 μm. (Inset) Higher magnification image of starter cell examples inside the region labeled by the dashed square.
(B) Same as (A) for rabies tracing experiments from SST-Nmbr interneurons in S1 and V1.
(C) Representative examples of rabies retrograde labeling from SST-Myh8 and SST-Nmbr interneurons in S1 and V1 using Neuroinfo 3D rendering. Magenta dots represent the location of rabies-traced presynaptic neurons.
(D) Presynaptic inputs to SST-Myh8 and SST-Nmbr interneurons in S1 quantified as the percentage of rabies traced cells in each regional category out of the total number of cells labeled in the brain (n = 3 for SST-Myh8, n = 2 for SST-Nmbr). The top 10 input regional categories for either SST subtype are included in the plot.
(E) One rabies tracing experiment of SST-Myh8 interneurons using the same AAV-helper viruses used for rabies tracing experiments from SST-Nmbr interneurons. (top) Schematics of experimental design. The construct of AAV-DIO-helper viruses and the timeline of AAV-helpers and N2cRV injections for tracing from SST-Myh8 in S1 using *Chrna2-Cre* mouse line are illustrated. Rabies tracing patterns were analyzed 15 days post-infection. (bottom left) Representative image showing the starter cells. (bottom right) Presynaptic inputs identified were quantified as the percentage of rabies-traced cells in each regional category out of the total number of presynaptic neurons labeled in the brain. Top 10 input regional categories are included in the plot.
Abbreviations for thalamic regions: ventral anterior-lateral complex of the thalamus (VAL), ventral posterolateral nucleus of the thalamus (VPL), ventral posteromedial nucleus of the thalamus (VPM), posterior complex of the thalamus (PO), reticular nucleus of the thalamus (RT).

SST-Myh8 rabies

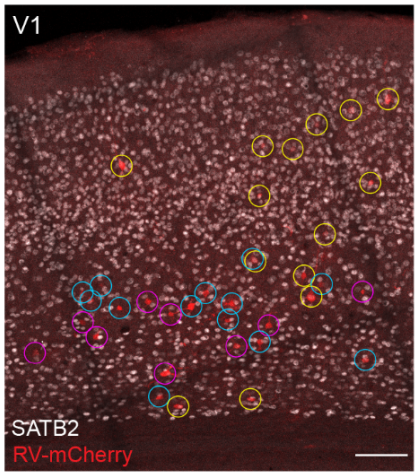

SATB2^{+} presynaptic neurons

SATB2^{-} presynaptic neurons

starter cells

SST-Nmbr rabies

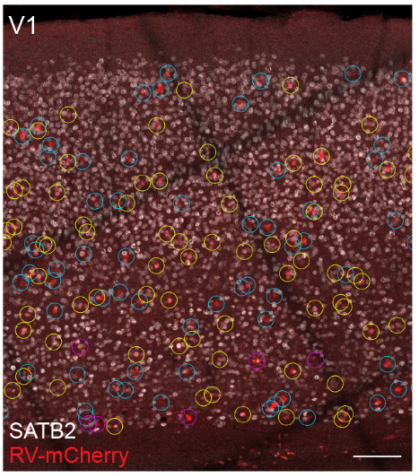

S1 exp#1

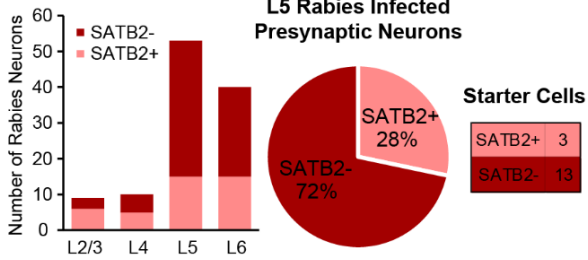

S1 exp#1

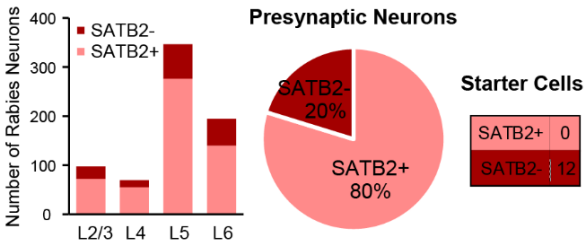

S1 exp#2

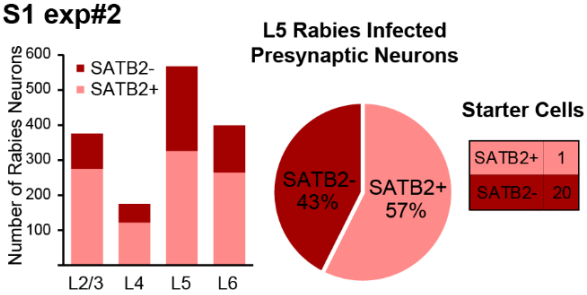

S1 exp#2

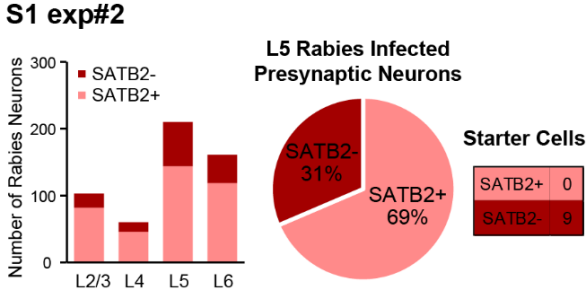

V1 exp#2

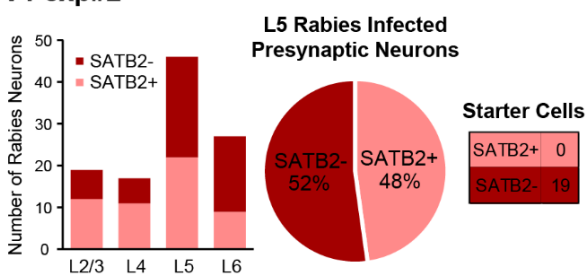

V1 exp#2

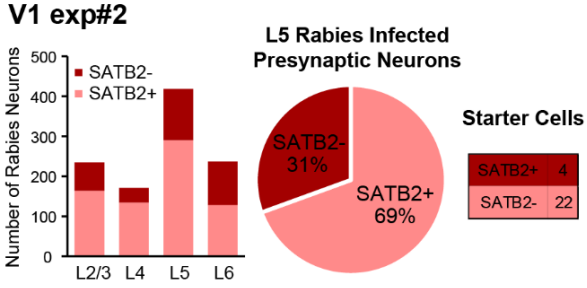

V1 exp#3

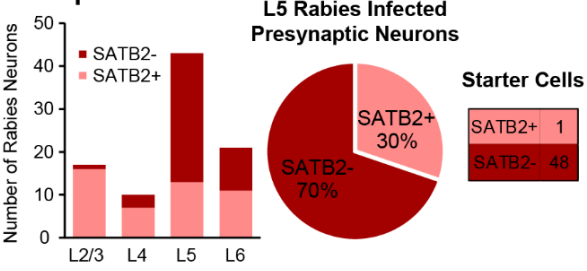

Figure S8. The identity of rabies-traced local presynaptic neurons to two SST subtypes. Related to Figure 6.

(left column from top to bottom) Representative image of immunostaining against SATB2 (white) on a brain slice with rabies traced presynaptic neurons (red) targeting SST-Myh8 interneurons in V1. Yellow circles indicate SATB2+ rabies traced presynaptic neurons. Cyan circles indicate SATB2- rabies traced presynaptic neurons. Magenta circles indicate starter cells. Quantification from individual rabies tracing experiments is shown below. For each experiment, a histogram of rabies traced neurons in each layer (left); a pie chart of the numbers of SATB2+ versus SATB2- rabies infected presynaptic neurons in L5 (middle), and a table shows the number of starter cells (right) are shown. Note that there are occasionally a small number of SATB2+ pyramidal neuron starter cells, due to the challenge of specifically targeting a small interneuron population that only constitutes ~2% of all cortical neurons. (right column) same elements for rabies tracing experiments from SST-Nmbr interneurons.

Table S7. Summary of data and statistical analysis. Related to Figure 3-5, 7.

Figure Panel	N	Statistical Test	P value
Figure 3C	L2/3: n = 8, 3 mice L5a: n = 8, 4 mice L5b: n = 18, 6 mice L6: n = 17, 5 mice total 6 mice	Linear mixed model with fixed factor only and multiple comparison with Bonferroni adjustment (test a) Kruskal-Wallis test with Dunn's correction (test b) (Note that linear mixed model with animal ID as random factor showed animal ID as a redundant factor)	Type III of fixed effect [Cortical Layer], p = .050; Estimates of fixed effect L5b, p = .009 (test a) L5b vs L6, p = .0178 (test b)
Figure 3D	L2/3: n = 12, 7 mice L5a: n = 24, 8 mice L5b: n = 24, 9 mice L6: n = 10, 4 mice total 12 mice	linear mixed model with animal ID as random factor and multiple comparison with Bonferroni adjustment	Type III of fixed effect [Cortical Layer], p < .001 Estimates of fixed effect: L5a p = .012 Pairwise comparison: L2/3 vs L5a, p < .001 L2/3 vs L5b, p < .001 L2/3 vs L6, p < .001 L5a vs L5b, p = .008
Figure 3E	L2/3: n = 8, 5 mice L5a: n = 20, 7 mice L5b: n = 23, 7 mice L6: n = 8, 5 mice total 10 mice	linear mixed model with animal ID as random factor and multiple comparison with Bonferroni adjustment	Type III of fixed effect [Cortical Layer], p = .047 Estimates of fixed effect: L5b, p = .025
Figure 3F	L2/3: n = 10, 6 mice L5a: n = 14, 5 mice L5b: n = 20, 6 mice L6: n = 13, 5 mice total 12 mice	linear mixed model with animal ID as random factor	Type III of fixed effect [Cortical Layer], p = .056 Estimates of fixed effect, n.s.
Figure 4D	pan-SST to IT neurons: n = 11, 3 mice PT neurons: n = 14, 3 mice	nested t-test	p = .0018
Figure 4E	SST-Calb2 to IT neurons: n = 21, 5 mice PT neurons: n = 14, 3 mice	nested t-test on rank transformed data	p = .0026
Figure 4F	SST-Myh8 to IT neurons n = 20, 4 mice PT neurons n = 25, 4 mice	nested t-test on rank transformed data	p = .0442
Figure 4G	SST-Nmbr to IT neurons n = 16, 3 mice PT neurons n = 14, 3 mice	nested t-test on rank transformed data	p = .0048
Figure 4I	See above	Kruskal-Wallis test with Dunn's correction for multiple comparisons	pan-SST vs. SST-Calb2 p < .0001 pan-SST vs. SST-Myh8 p = .0002 pan-SST vs. SST-Nmbr p = .0254 SST-Calb2 vs. SST-Nmbr p = .0288

Figure 4J	See above	Kruskal-Wallis test with Dunn's correction for multiple comparisons	pan-SST vs. SST-Calb2 p = .0515 pan-SST vs. SST-Myh8 p = .0033 pan-SST vs. SST-Nmbr p < .0001 SST-Calb2 vs. SST-Nmbr p = .0005 SST-Myh8 vs SST-Nmbr p = .0004
Figure 5D	SST-Calb2 to PV L2/3: n = 9, L5/6: n = 11, 3 mice SST-Myh8 to PV L2/3: n = 9, L5/6: n = 13, 3 mice SST-Nmbr to PV L2/3: n = 8, L5/6: n = 17, 4 mice	linear mixed model with animal ID as the random factor	SST-Calb2: L2/3 PV vs L5/6 PV p = .006 SST-Myh8: L2/3 PV vs L5/6 PV p = .088 SST-Nmbr: L2/3 PV vs L5/6 PV p = .127 p values reflect both type III test of fixed effect and estimates of fixed effect
Figure 5E	See above	Kruskal-Wallis test	Output to L2/3 PV: SST-Calb2 vs SST-Myh8 p = .0062 SST-Calb2 vs SST-Nmbr p = .0005
Figure 7F	SST-Calb2 puncta on L5-PT dendritic compartments tuft n = 16 ROIs apical branch n = 16 ROIs trunk n =23 ROIs oblique n = 25 ROIs basal n = 15 ROIs total 3 mice	Linear mixed model with fixed factor only and multiple comparison with Bonferroni adjustment (Note that Linear mixed model using dendritic compartment as fixed factor and animal ID as random factor showed animal ID is a redundant factor)	Type III tests of fixed effect [Dendritic Compartments], p < .001 Estimates of fixed effects: trunk p = .011, oblique p < .001, basal p < .001 Pairwise comparison: tuft vs. oblique p = .002 tuft vs. basal p < .001 apical branch vs. basal p = .006 apical branch vs. oblique p = .039
Figure 7G	SST-Myh8 puncta on L5-PT dendritic compartments tuft n = 18 ROIs apical branch n = 25 ROIs trunk n = 17 ROIs oblique n = 16 ROIs basal n = 18 ROIs total 3 mice	Linear mixed model with fixed factor only and multiple comparison with Bonferroni adjustment (Note that Linear mixed model using dendritic compartment as fixed factor and animal ID as random factor showed animal ID is a redundant factor)	Type III tests of fixed effect [Dendritic Compartments], p < .001 Estimates of fixed effects: apical branch p < .001, trunk p < .001, oblique p < .001, basal p < .001 Pairwise comparison: tuft vs. apical branch p < .001 tuft vs. trunk p < .001 tuft vs. oblique p< .001 tuft vs. basal p < .001
Figure 7H	See above	Mann-Whitney test	SST-Calb2 vs SST-Myh8 on tuft p = .0001 apical branch p < .0001 trunk p = .0103 oblique p = .0016 basal p = .0396